Maximum Likelihood Analysis of the RVoG Model for Forestry Studies in PolInSAR

Carlos López-Martínez, Xavier Fàbregas, Alberto Alonso-González

→ POLINSAR 2013

January 2013
Fracati, ITALY

Universitat Politècnica de Catalunya – UPC
Signal Theory and Communications Dept.
Barcelona, Spain
carlos.lopez@tsc.upc.edu

Table of Contents

- RVoG/Line model
- Coherence Linearity Hypothesis
- Validation and Estimation based on the RVoG/Line model
  - SB-PolInSAR
  - MB-PolInSAR
- Results & Comparison at P&L-band data
- Conclusions

Random Volume over Ground RVoG scattering model or Line model

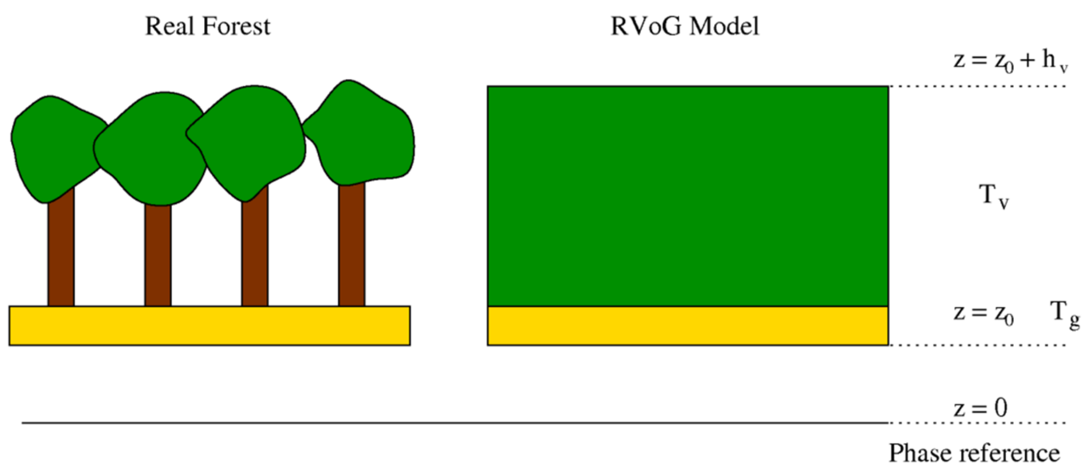

PolInSAR coherency matrix

$$\mathbf{T} = \begin{bmatrix} \mathbf{T}_{11} & \mathbf{\Omega}_{12} & \cdots & \mathbf{\Omega}_{1N} \\ \mathbf{\Omega}_{21} & \mathbf{T}_{22} & & \\ \vdots & & \ddots & \\ \mathbf{\Omega}_{N1} & & & \mathbf{T}_{NN} \end{bmatrix}$$

Interferometric coherence as a function of polarization **w**

- Describes a line in the complex plane

$$\rho(\mathbf{w}) = e^{j\phi_0}\left(\rho_{vol} + \frac{\mu(\mathbf{w})}{1+\mu(\mathbf{w})}(1-\rho_{vol})\right)$$

  - Slope: Baseline, Veg. height, extinction, ground phase
  - Length: Baseline, veg. height, extinction, Ground-to-Volume ratio $\mu(\mathbf{w})$

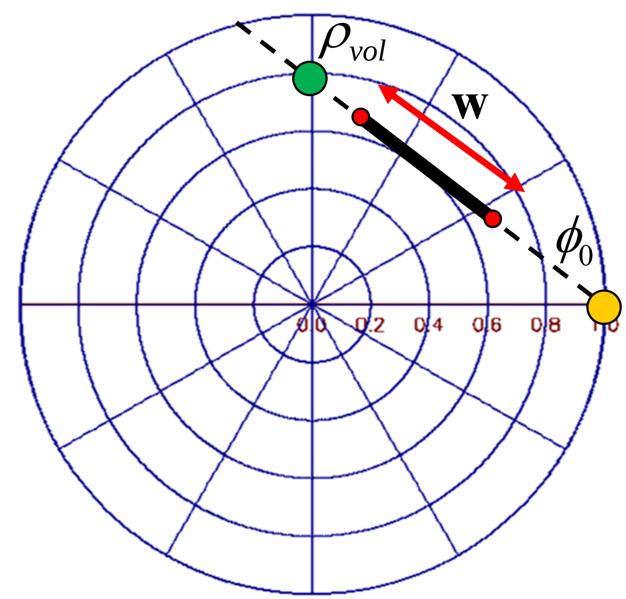

Polarimetric SAR Interferometry Statistics

Statistical description of SB-PolInSAR data. Extention to MB-PolInSAR is straightforward

$$\mathbf{k}_{p,1} = \frac{1}{\sqrt{2}}\begin{bmatrix} S_{hh,1}+S_{vv,1} \\ S_{hh,1}-S_{vv,1} \\ 2S_{hv,1} \end{bmatrix} \qquad \mathbf{k}_{p,2} = \frac{1}{\sqrt{2}}\begin{bmatrix} S_{hh,2}+S_{vv,2} \\ S_{hh,2}-S_{vv,2} \\ 2S_{hv,2} \end{bmatrix}$$

$$\Rightarrow \quad \mathbf{k} = \begin{bmatrix} \mathbf{k}_{p,1} \\ \mathbf{k}_{p,2} \end{bmatrix} \quad \Rightarrow$$

$$\mathbf{T} = E\left\{\mathbf{k}\mathbf{k}^H\right\} = \begin{bmatrix} \mathbf{T}_{11} & \mathbf{\Omega}_{12} \\ \mathbf{\Omega}_{12}^H & \mathbf{T}_{22} \end{bmatrix}$$

$$\mathbf{T} = \begin{bmatrix} \mathbf{T}_{11}^{1/2} & 0 \\ 0 & \mathbf{T}_{22}^{1/2} \end{bmatrix}\begin{bmatrix} \mathbf{I} & \tilde{\mathbf{\Omega}}_{12} \\ \tilde{\mathbf{\Omega}}_{12}^H & \mathbf{I} \end{bmatrix}\begin{bmatrix} \mathbf{T}_{11}^{1/2} & 0 \\ 0 & \mathbf{T}_{22}^{1/2} \end{bmatrix}$$

PolInSAR
coherency matrix

Multidimensional, zero-mean, complex Gaussian/Wishart PDF

$$\mathbf{k} = \begin{bmatrix} S_1 \\ S_2 \\ \vdots \\ S_m \end{bmatrix}$$

$$S_k = \mathrm{N}_{C^2}\left(0, \sigma^2/2\right)$$

$$\boxed{\mathbf{Z} = \frac{1}{n}\sum_{i=1}^{n}\mathbf{k}_i\mathbf{k}_i^H}$$

$$\mathbf{Z} \sim \mathrm{W}\left(n, \mathbf{T}\right)$$

Wishart PDF

$$p_{\mathbf{Z}}\left(\mathbf{Z}\right) = \frac{n^{mn}\left|\mathbf{Z}\right|^{n-m}}{\left|\mathbf{T}\right|^{n}\tilde{\Gamma}_m\left(n\right)}\mathrm{etr}\left(-n\mathbf{T}^{-1}\mathbf{Z}\right)$$

Limitations $\begin{cases} \mathbf{Z} \quad \mathbf{T} & \text{Positive definite} \\ n \geq m & \end{cases}$

RVoG Model

Conditions imposed by the RVoG model on the data, i.e., coherency matrix

- Polarimetric stationarity hypothesis (PS)

$$\rho_v = e^{j\phi_0} \frac{\int_0^{h_v} F(z) e^{jk_z z} dz}{\int_0^{h_v} F(z) dz} \Rightarrow \boxed{\mathbf{T}_{11} = \mathbf{T}_{22}} \Rightarrow \rho(\mathbf{w}) = \frac{\mathbf{w}^H \mathbf{\Omega}_{12} \mathbf{w}}{\mathbf{w}^H \mathbf{T}_{11} \mathbf{w}}$$

- Interferometrically polarimetric stationarity hypothesis (IPS)

$$\tilde{\mathbf{\Omega}}_{12} = \mathbf{U} \mathbf{\Lambda} \mathbf{U}^H \Rightarrow \boxed{\tilde{\mathbf{\Omega}}_{12}^H \tilde{\mathbf{\Omega}}_{12} = \tilde{\mathbf{\Omega}}_{12} \tilde{\mathbf{\Omega}}_{12}^H}$$

$\tilde{\mathbf{\Omega}}_{12}$ is a normal matrix

- Coherence linearity (CL)
  - $\rho(\mathbf{w})$ presents a linear behavior wrt **w** in the complex plane
  - Does not result from PS and IPS hypotheses

Question: How to relate the CL hypothesis with a property of the coherency matrix?

Coherence Linearity Hypothesis

How to consider the CL hypothesis in terms of the coherency matrix ?

- Mathematical conditions imposed in the coherency matrix by CL

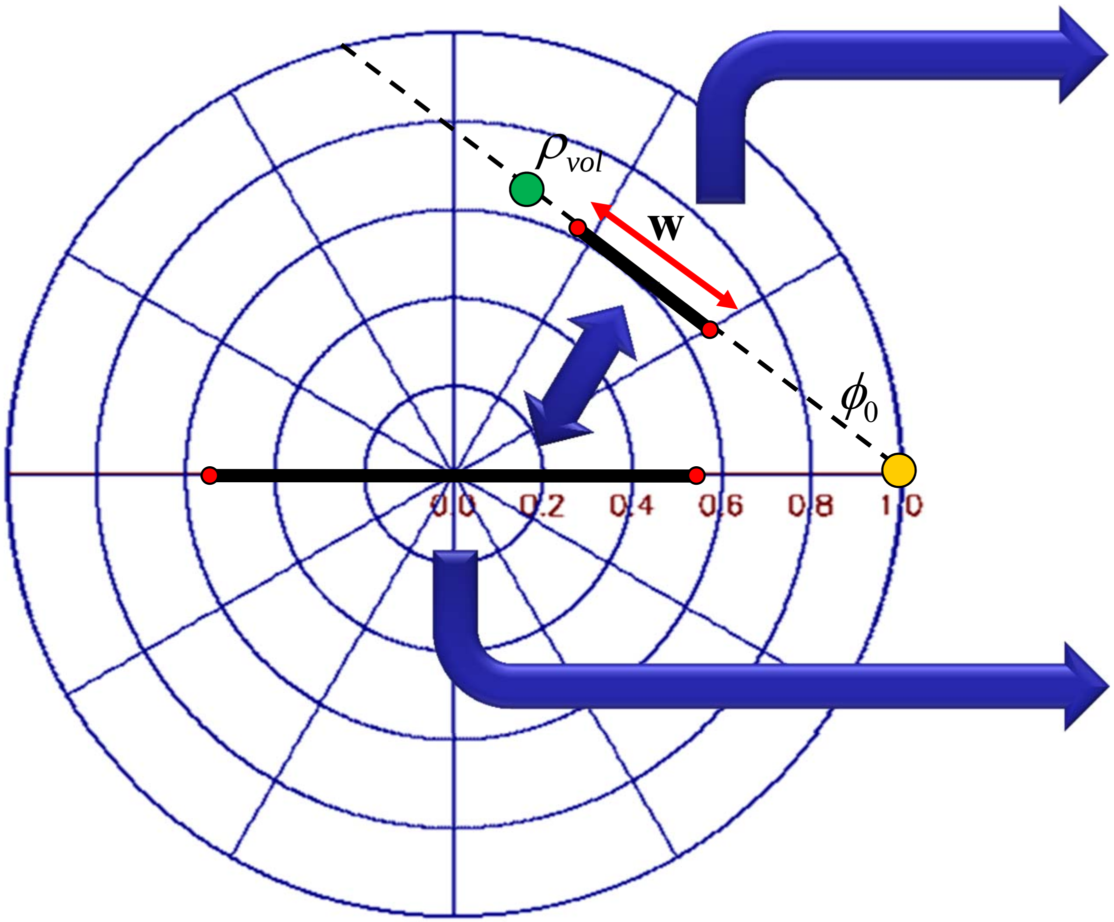

Depends on $\mathbf{\Omega}_{12}$ or $\tilde{\mathbf{\Omega}}_{12}$

Complex coherence $\rho(\mathbf{w})$ as a function of **w**

Hermitian matrices present real eigenvalues that describe a line

CL is related with the property of Hemiticity of a matrix

- For real PolInSAR data, in presence of speckle, the transform needs to be more general than translations and rotations

Numerical Range

The interferometric coherence can be explored in terms of the numerical range of the matrix $\tilde{\mathbf{\Omega}}_{12}$

$$W\left(\tilde{\mathbf{\Omega}}_{12}\right)=\left\{\mathbf{v}^H\tilde{\mathbf{\Omega}}_{12}\mathbf{v}, \mathbf{v}\in\mathbb{C}^3, \mathbf{v}^H\mathbf{v}=1\right\}$$

For a given complex matrix **A** and a unitary vector $\mathbf{x}^H\mathbf{x}=1$

$$\mathbf{H}_1=\frac{\mathbf{A}+\mathbf{A}^H}{2}$$ Hermitian part

$$\mathbf{H}_2=\frac{\mathbf{A}-\mathbf{A}^H}{2j}$$ Non-Hermitian part

$$\mathbf{A}=\mathbf{H}_1+j\mathbf{H}_2$$

$\Rightarrow$

$$\Re\left\{W\left(\mathbf{A}\right)\right\}=\mathbf{x}^H\mathbf{H}_1\mathbf{x}$$

$$\Im\left\{W\left(\mathbf{A}\right)\right\}=\mathbf{x}^H\mathbf{H}_2\mathbf{x}$$

$\Rightarrow$ If $\Im\left\{W\left(\mathbf{A}\right)\right\}=0$ $\mathbf{H}_2=\mathbf{0}$, then $W\left(\mathbf{A}\right)$ is a line in the real axis

If **A** is an Hermitian matrix, $W\left(\mathbf{A}\right)$ is a line in the real axis, so the interferometric coherence describes a line and the CL hypothesis applies

In general, $\tilde{\mathbf{\Omega}}_{12}$ is a non-Hermitian matrix

Affine Transformation in the Complex Plane

In geometry, an affine transformation is a transformation which preserves straight lines and ratios of distances between points lying on a straight line. It does not necessarily preserve angles or lengths

- Translation, geometric contraction, expansion, dilation, reflection, rotation, shear, similarity transformations, and spiral similarities

Affine transformations allow to transform straight lines in the complex plane

$$\tau_{abc}(\rho) = a\Re\{\rho\} + jb\Im\{\rho\} + c, \quad \{a,b,c\} \in \mathbb{C}$$

$$\tau_{abc}(\rho) = a\mathbf{x}^H\mathbf{H}_1\mathbf{x} + jb\mathbf{x}^H\mathbf{H}_2\mathbf{x} + c$$

$$\tau_{abc}(\mathbf{A}) = a\mathbf{H}_1 + jb\mathbf{H}_2 + c\mathbf{I} = \mathbf{A}^\tau = \mathbf{H}_1^\tau + j\mathbf{H}_2^\tau$$

Affine equivalent matrices

$\{a,b,c\}$ such that $\tau_{abc}(\rho) \in \Re$

$\mathbf{A}^\tau$ is an Hermitian matrix

The numerical range of a matrix **A** is a line segment in the complex plane if it is affine equivalent to an Hermitian matrix. In terms of the interferometric coherence, it describes a line in the complex plane

Affine Transformation in the Complex Plane

Affine and Inverse Affine transformation maps

$$
\begin{array}{ccc}
\mathbf{A} = \mathbf{H}_1 + j\mathbf{H}_2 & \underset{AT}{\overset{\tau_{abc}}{\rightarrow}} & \mathbf{A}^\tau = a\mathbf{H}_1 + jb\mathbf{H}_2 + c\mathbf{I} \\
\uparrow & & \downarrow \\
\mathbf{A} = a'\mathbf{H}_1^\tau + jb'\mathbf{H}_2^\tau + c'\mathbf{I} & \underset{\tau_{abc}^{-1}=\tau_{a'b'c'}}{\overset{IAT}{\leftarrow}} & \mathbf{A}^\tau = \mathbf{H}_1^\tau + j\mathbf{H}_2^\tau
\end{array}
$$

The transform coefficients $\{a,b,c\} \in \mathbb{R}$ can be obtained by considering

$$\tilde{\mathbf{\Omega}}_{12} = a'\mathbf{H}_1^\tau + jb'\mathbf{H}_2^\tau + c'\mathbf{I} \Rightarrow \mathbf{H}_2^\tau = \mathbf{0}$$

$$\Rightarrow \mathbf{H}_2^\tau = \frac{\tilde{\mathbf{\Omega}}_{12}^\tau - \tilde{\mathbf{\Omega}}_{12}^{\tau\,H}}{2j} = \frac{\left(a\mathbf{H}_1 + jb\mathbf{H}_2 + c\mathbf{I}\right) - \left(a\mathbf{H}_1 + jb\mathbf{H}_2 + c\mathbf{I}\right)^H}{2j} = \mathbf{0}$$

- In absence of speckle noise, $\{a,b,c\} \in \mathbb{R}$ can be obtained and define a line transformation
- In presence of speckle noise, there is no solution for $\{a,b,c\} \in \mathbb{R}$, but the following minimization can be adopted. It defines a general affine transformation

$$a,b,c = \arg\min_{a,b,c} \left|\mathbf{v}^H \mathbf{H}_2^\tau \mathbf{v}\right|$$

$$\left|\mathbf{v}^H \mathbf{H}_2^\tau \mathbf{v}\right|^2 \leq \left\|\mathbf{H}_2^\tau\right\|_2$$

$$\Rightarrow a,b,c = \arg\min_{a,b,c} \left\|\mathbf{H}_2^\tau\right\|_2 = \arg\min_{a,b,c} \operatorname{tr}\left(\mathbf{H}_2^{\tau\,H}\mathbf{H}_2^\tau\right)$$

Maximum Likelihood Analysis of the RVoG

The numerical range of a matrix **A** is a line segment in the complex plane if it is affine equivalent to an Hermitian matrix. In terms of the interferometric coherence, it describes a line in the complex plane

- General structure of the coherency matrix

$$\mathbf{T} = \begin{bmatrix} \mathbf{T}_{11} & \boldsymbol{\Omega}_{12} \\ \boldsymbol{\Omega}_{12}^{H} & \mathbf{T}_{22} \end{bmatrix}$$

- Based on the Affine Transformation it is possible to define the structure of the coherency matrix under the RVoG hypothesis

$$\mathbf{T}_{RVoG} = \begin{bmatrix} \mathbf{T}_{11} & \mathbf{T}_{11}^{1/2}\tilde{\boldsymbol{\Omega}}_{12}\mathbf{T}_{11}^{1/2} \\ \mathbf{T}_{11}^{1/2}\tilde{\boldsymbol{\Omega}}_{12}\mathbf{T}_{11}^{1/2} & \mathbf{T}_{11} \end{bmatrix} = \begin{bmatrix} \mathbf{T}_{11} & \mathbf{T}_{11}^{1/2}\left(a'\mathbf{H}_{1}^{\tau} + c'\mathbf{I}\right)\mathbf{T}_{11}^{1/2} \\ \mathbf{T}_{11}^{1/2}\left(a'\mathbf{H}_{1}^{\tau} + c'\mathbf{I}\right)\mathbf{T}_{11}^{1/2} & \mathbf{T}_{11} \end{bmatrix}$$

- Generalized Likelihood Ratio Test (GLRT) in the **original domain**

$$H_0 : \mathbf{T} = \mathbf{T}_{RVoG} \qquad H_1 : \mathbf{T}$$

$$\Rightarrow \quad \Lambda_{RVoG} = \frac{p_{\mathbf{Z}}\left(\mathbf{Z}; \hat{\mathbf{T}}_{RVoG}, H_0\right)}{p_{\mathbf{Z}}\left(\mathbf{Z}; \hat{\mathbf{T}}, H_1\right)} \underset{H_1}{\overset{H_0}{\gtrless}} \gamma$$

Maximum Likelihood Analysis of the RVoG

In the original domain, the GLRT must estimate: $\left\{\mathbf{T}_{11}, \mathbf{H}_1^{\tau}, a', c'\right\}$

If the estimation is considered in the affined transformed domain

- General structure of the coherency matrix

$$\mathbf{T}^{\tau} = \begin{bmatrix} \mathbf{T}_{11} & \mathbf{T}_{11}^{1/2}\left(\mathbf{H}_1^{\tau} + j\mathbf{H}_2^{\tau}\right)\mathbf{T}_{22}^{1/2} \\ \mathbf{T}_{11}^{1/2}\left(\mathbf{H}_1^{\tau} + j\mathbf{H}_2^{\tau}\right)\mathbf{T}_{22}^{1/2} & \mathbf{T}_{22} \end{bmatrix}$$

- Structure of the coherency matrix under the RVoG hypothesis

$$\mathbf{T}_{RVoG}^{\tau} = \begin{bmatrix} \mathbf{T}_{11} & \mathbf{T}_{11}^{1/2}\mathbf{H}_1^{\tau}\mathbf{T}_{11}^{1/2} \\ \mathbf{T}_{11}^{1/2}\mathbf{H}_1^{\tau}\mathbf{T}_{11}^{1/2} & \mathbf{T}_{11} \end{bmatrix} = \begin{bmatrix} \mathbf{T}_{11} & \mathbf{\Omega}_{12}^{\tau} \\ \mathbf{\Omega}_{12}^{\tau} & \mathbf{T}_{11} \end{bmatrix}$$

- Generalized Likelihood Ratio Test (GLRT) in the **transformed domain**

$$H_0 : \mathbf{T} = \mathbf{T}_{RVoG}$$
$$H_1 : \mathbf{T}$$

$$\Rightarrow \quad \Lambda_{RVoG}^{\tau} = \frac{p_{\mathbf{Z}}\left(\mathbf{Z}^{\tau}; \hat{\mathbf{T}}_{RVoG}^{\tau}, H_0\right)}{p_{\mathbf{Z}}\left(\mathbf{Z}^{\tau}; \hat{\mathbf{T}}^{\tau}, H_1\right)} \underset{H_1}{\overset{H_0}{\gtrless}} \gamma$$

Calculation of the Generalized Likelihood Ratio Test

Maximized $\mathbf{Z}^{\tau}_{RVoG} = \begin{bmatrix} \dfrac{\mathbf{Z}_{11}+\mathbf{Z}_{22}}{2} & \dfrac{\mathbf{Z}^{\tau}_{12}+\left(\mathbf{Z}^{\tau}_{12}\right)^{H}}{2} \\ \dfrac{\mathbf{Z}^{\tau}_{12}+\left(\mathbf{Z}^{\tau}_{12}\right)^{H}}{2} & \dfrac{\mathbf{Z}_{11}+\mathbf{Z}_{22}}{2} \end{bmatrix}$

$$\Lambda^{\tau}_{RVoG} = \frac{p_{\mathbf{Z}}\left(\mathbf{Z}^{\tau};\hat{\mathbf{T}}^{\tau}_{RVoG},H_0\right)}{p_{\mathbf{Z}}\left(\mathbf{Z}^{\tau};\hat{\mathbf{T}}^{\tau},H_1\right)} \underset{H_1}{\overset{H_0}{\gtrless}} \gamma$$

$$\Lambda^{\tau}_{RVoG} = \left(\frac{\left|\mathbf{Z}^{\tau}\right|}{\left|\mathbf{Z}^{\tau}_{RVoG}\right|}\right)^{n} = \left(\frac{\left|\mathbf{Z}_{11}\right|\left|\mathbf{Z}_{22}\right|}{\left|\dfrac{\mathbf{Z}_{11}+\mathbf{Z}_{22}}{2}\right|^{2}}\right)^{n} \left(\frac{\left|\mathbf{I}-\tilde{\mathbf{Z}}^{\tau}_{12}\tilde{\mathbf{Z}}^{\tau}_{21}\right|}{\left|\mathbf{I}-\tilde{\mathbf{Z}}^{\tau}_{12,RVoG}\tilde{\mathbf{Z}}^{\tau}_{21,RVoG}\right|}\right)^{n}$$

PS hypothesis Λ^{τ}_{PS}

CL hypothesis Λ^{τ}_{CL}

Maximized $\mathbf{Z}^{\tau} = \begin{bmatrix} \mathbf{Z}_{11} & \mathbf{Z}^{\tau}_{12} \\ \left(\mathbf{Z}^{\tau}_{12}\right)^{H} & \mathbf{Z}_{22} \end{bmatrix}$

Maximum Likelihood Analysis of the RVoG

The MLE estimation of the covariance matrix under the RVoG model assumptiom is obtained in the transformed domain by the affine transformation

$$\mathbf{Z}^{\tau}_{RVoG} = \begin{bmatrix} \dfrac{\mathbf{Z}_{11}+\mathbf{Z}_{22}}{2} & \dfrac{\mathbf{Z}^{\tau}_{12}+\left(\mathbf{Z}^{\tau}_{12}\right)^{H}}{2} \\ \dfrac{\mathbf{Z}^{\tau}_{12}+\left(\mathbf{Z}^{\tau}_{12}\right)^{H}}{2} & \dfrac{\mathbf{Z}_{11}+\mathbf{Z}_{22}}{2} \end{bmatrix}$$

To obtain the estimated coherency matrix in the original domain, the inverse affine transformation must be applied

$$\mathbf{Z}_{RVoG} = \begin{bmatrix} \dfrac{\mathbf{Z}_{11}+\mathbf{Z}_{22}}{2} & \left(\dfrac{\mathbf{Z}_{11}+\mathbf{Z}_{22}}{2}\right)^{\frac{1}{2}}\left(a'\left(\dfrac{\tilde{\mathbf{Z}}^{\tau}_{12}+\left(\tilde{\mathbf{Z}}^{\tau}_{12}\right)^{H}}{2}\right)+c'\mathbf{I}_3\right)\left(\dfrac{\mathbf{Z}_{11}+\mathbf{Z}_{22}}{2}\right)^{\frac{1}{2}} \\ \left(\left(\dfrac{\mathbf{Z}_{11}+\mathbf{Z}_{22}}{2}\right)^{\frac{1}{2}}\left(a'\left(\dfrac{\tilde{\mathbf{Z}}^{\tau}_{12}+\left(\tilde{\mathbf{Z}}^{\tau}_{12}\right)^{H}}{2}\right)+c'\mathbf{I}_3\right)\left(\dfrac{\mathbf{Z}_{11}+\mathbf{Z}_{22}}{2}\right)^{\frac{1}{2}}\right)^{H} & \dfrac{\mathbf{Z}_{11}+\mathbf{Z}_{22}}{2} \end{bmatrix}$$

Extension to MB-PolInSAR

Straightforward extension to MB-PolInSAR

- The previous analysis can be considered for all the $\mathbf{\Omega}_{ij}$ PolInSAR matrices, i.e, PolInSAR pairs

$$\mathbf{T} = \begin{bmatrix} \mathbf{T}_{11} & \mathbf{\Omega}_{12} & \cdots & \mathbf{\Omega}_{1N} \\ \mathbf{\Omega}_{21} & \mathbf{T}_{22} & & \\ \vdots & & \ddots & \\ \mathbf{\Omega}_{N1} & & & \mathbf{T}_{NN} \end{bmatrix} \Rightarrow \mathbf{Z} = \begin{bmatrix} \mathbf{Z}_{11} & \mathbf{Z}_{12} & \cdots & \mathbf{Z}_{1N} \\ \mathbf{Z}_{21} & \mathbf{Z}_{22} & & \\ \vdots & & \ddots & \\ \mathbf{Z}_{N1} & & & \mathbf{Z}_{NN} \end{bmatrix}$$

Unrestricted MLE

$$\mathbf{T}_{RVoG} = \begin{bmatrix} \mathbf{T}_{11} & \mathbf{\Omega}_{12} & \cdots & \mathbf{\Omega}_{1N} \\ \mathbf{\Omega}_{21} & \mathbf{T}_{11} & & \\ \vdots & & \ddots & \\ \mathbf{\Omega}_{N1} & & & \mathbf{T}_{11} \end{bmatrix} \Rightarrow \mathbf{Z}_{RVoG} = \begin{bmatrix} \mathbf{Z}_{Avg} & \mathbf{Z}_{12} & \cdots & \mathbf{Z}_{1N} \\ \mathbf{Z}_{21} & \mathbf{Z}_{Avg} & & \\ \vdots & & \ddots & \\ \mathbf{Z}_{N1} & & & \mathbf{Z}_{Avg} \end{bmatrix}$$

$$\mathbf{\Omega}_{ij} = \mathbf{T}_{11}^{1/2}\left(a'_{ij}\mathbf{H}^{\tau}_{1,ij} + c'_{ij}\mathbf{I}\right)\mathbf{T}_{11}^{1/2}$$

$$\mathbf{Z}_{ij} = \mathbf{Z}_{Avg}^{\frac{1}{2}}\left(a'_{ij}\left(\frac{\tilde{\mathbf{Z}}^{\tau}_{ij} + \left(\tilde{\mathbf{Z}}^{\tau}_{ij}\right)^{H}}{2}\right) + c'_{ij}\mathbf{I}_3\right)\mathbf{Z}_{Avg}^{\frac{1}{2}}$$

$$\mathbf{Z}_{Avg} = \frac{1}{N}\sum_{k=1}^{N}\mathbf{Z}_{kk}$$

Results: Real PolInSAR Data

PolInSAR data: E-SAR INDREX-II Campaign Tropical Forest

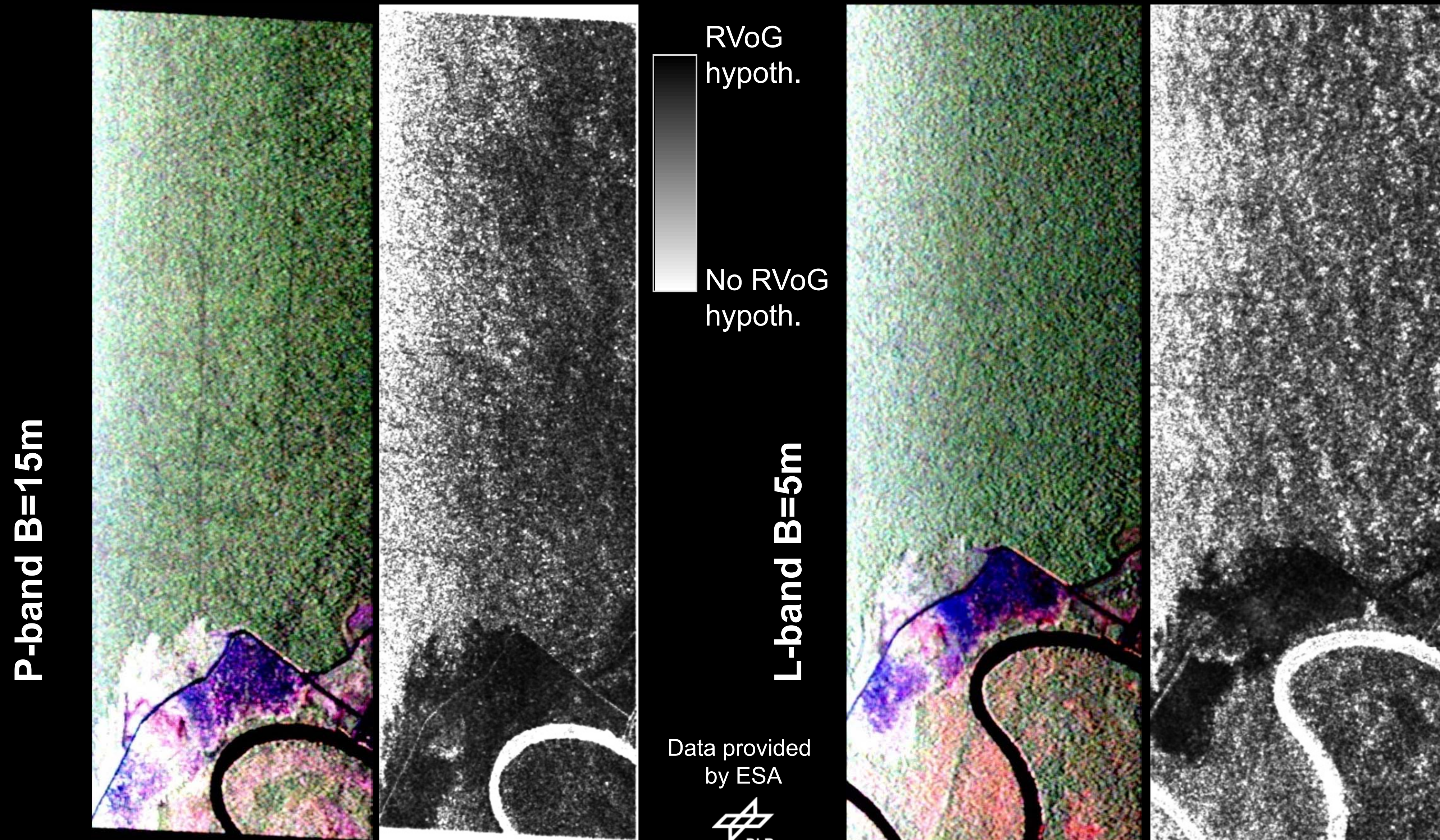

|HH+VV| |HV| |HH-VV| $-2\ln\left(\Lambda_{RVoG}^{\tau}\right)$ |HH+VV| |HV| |HH-VV| $-2\ln\left(\Lambda_{RVoG}^{\tau}\right)$

Results: Real PolInSAR Data

PolInSAR data: E-SAR INDREX-II Campaign Tropical Forest

P-band

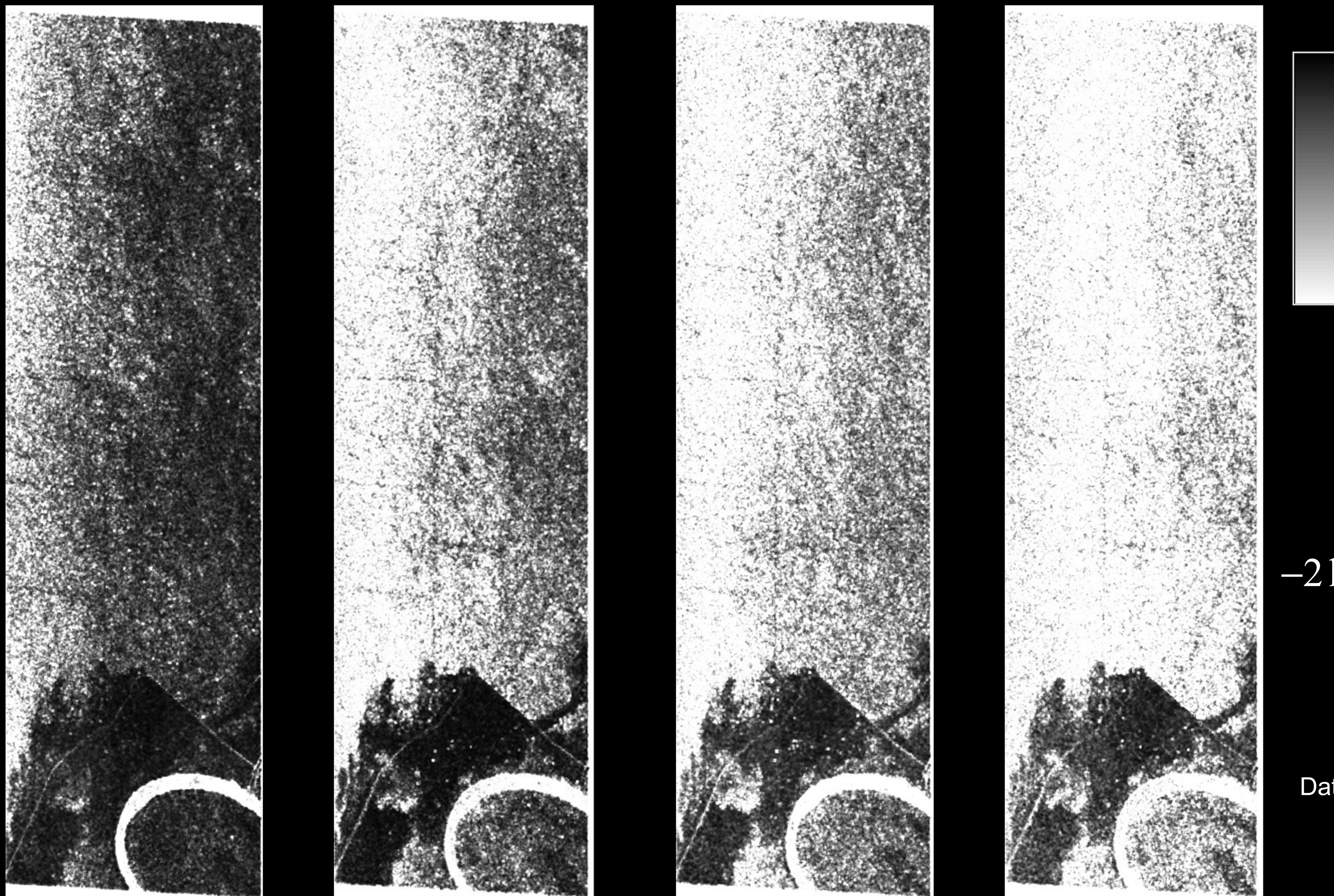

B=15m B=25m B=30m B=40m

$$-2\ln\left(\Lambda^{\tau}_{RVoG}\right)$$

Data provided by ESA

Results: Real PolInSAR Data

PolInSAR data: E-SAR INDREX-II Campaign Tropical Forest

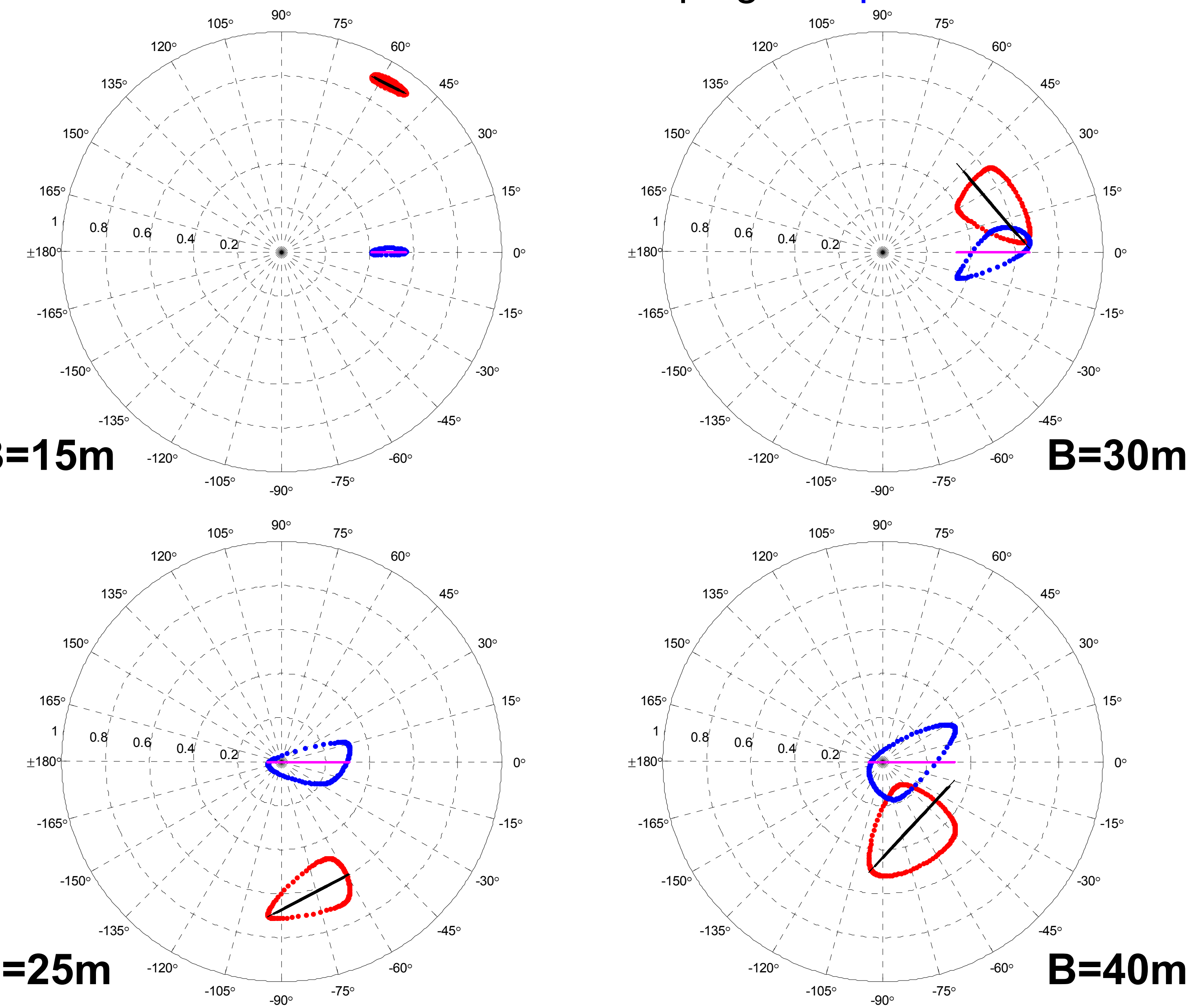

The four CRs refer to the same pixel

Estimated CR from multilook

Estimated CR from ML

Estimated CR from multilook (transformed)

Estimated CR from ML (transformed)

© Carlos López-Martínez, 2013, UPC-RSLab, carlos.lopez@tsc.upc.edu

Results: Real PolInSAR Data

PolInSAR data: E-SAR INDREX-II Campaign Tropical Forest

L-band

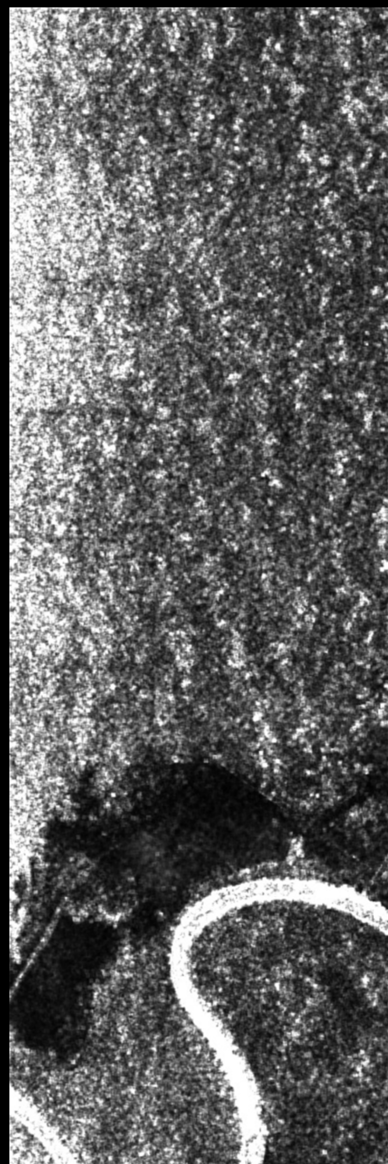

B=5m

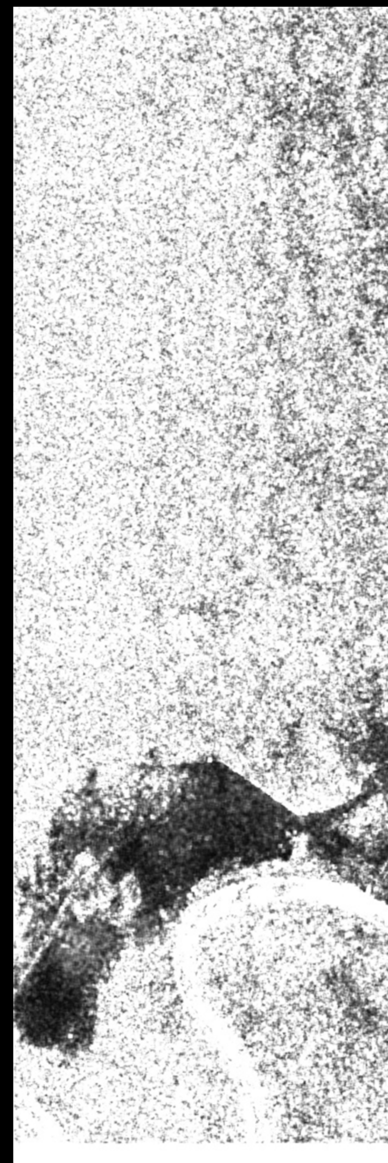

B=15m

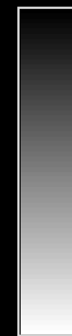

RVoG hypoth.

No RVoG hypoth.

$$-2\ln\left(\Lambda^{\tau}_{RVoG}\right)$$

Data provided by ESA

DLR

Results: Real PolInSAR Data

PolInSAR data: E-SAR INDREX-II Campaign Tropical Forest

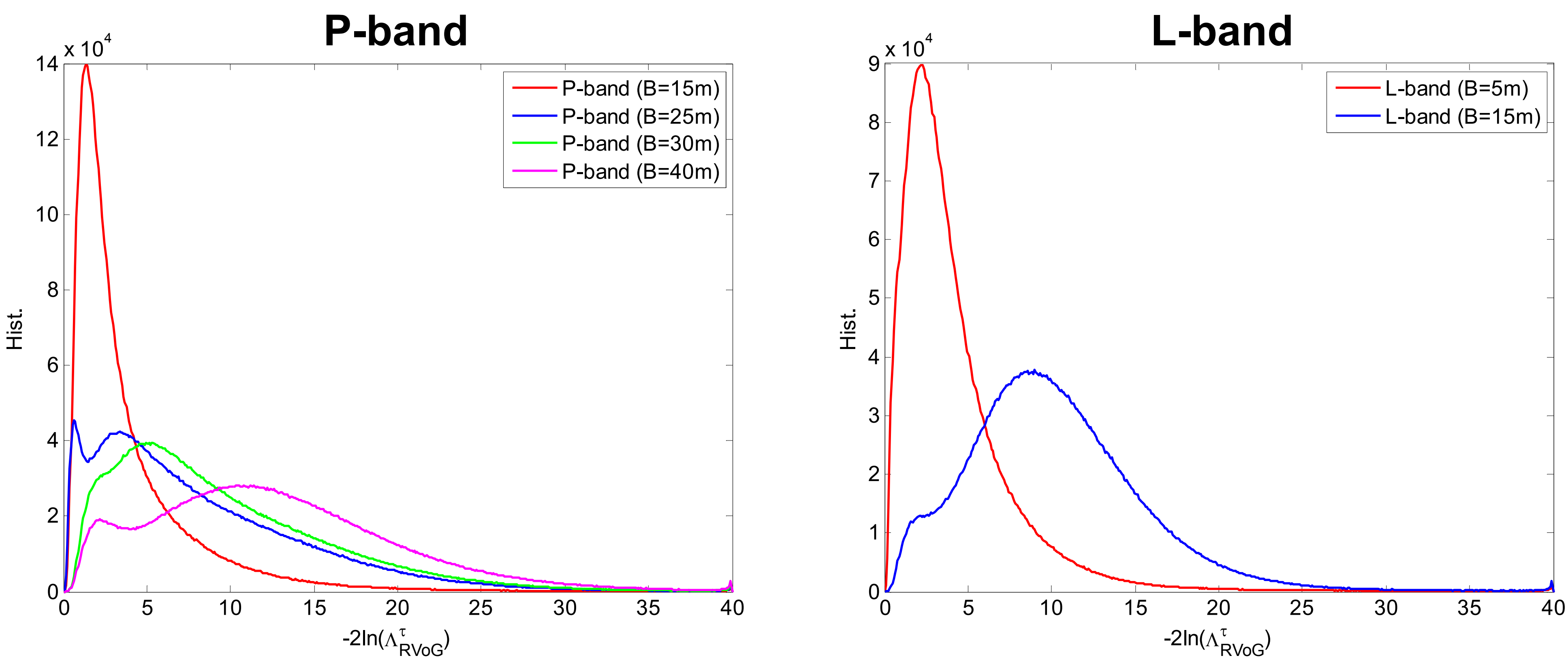

- The validity of the RVoG model hypothesis depends on the spatial baseline

Results: Real PolInSAR Data

PolInSAR data: E-SAR INDREX-II Campaign Tropical Forest

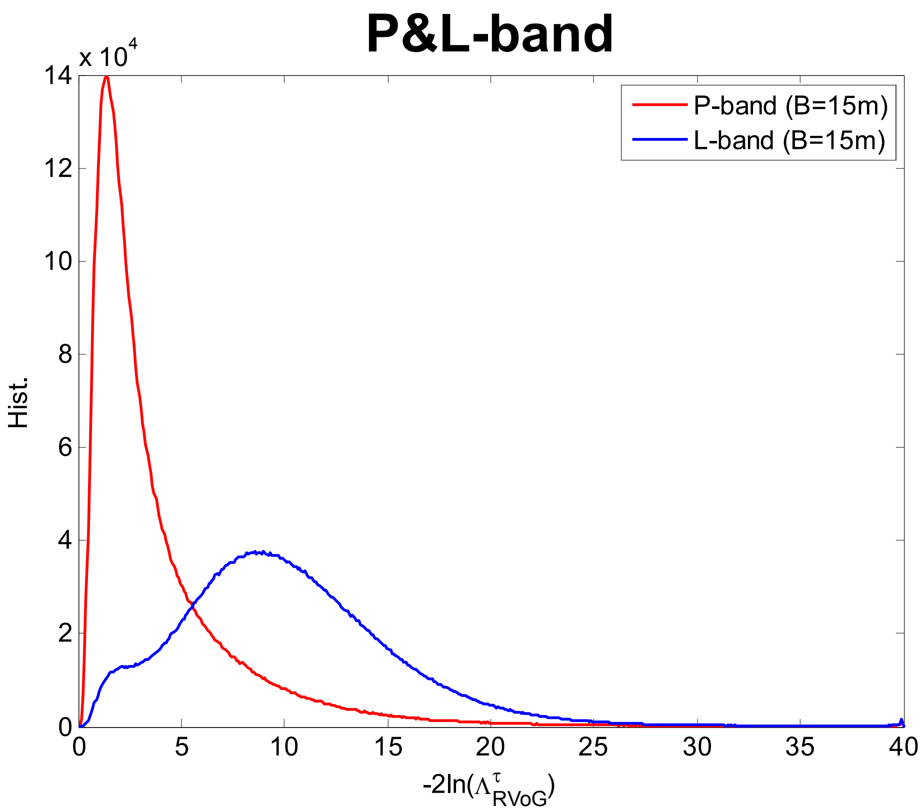

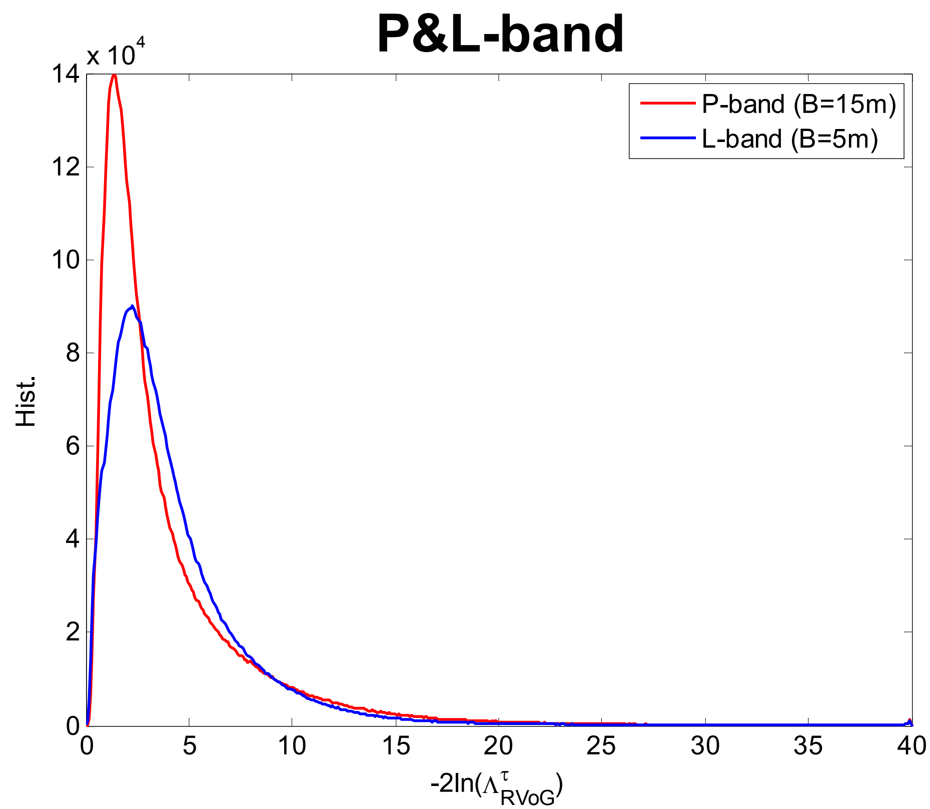

- The validity of the RVoG model hypothesis is equal at P- and L-bands, but considering different baselines. In the same conditions, the validity is larger at P-band

Results: Real PolInSAR Data

PolInSAR data: E-SAR BioSAR-1 Campaign Boreal Forest

P-band

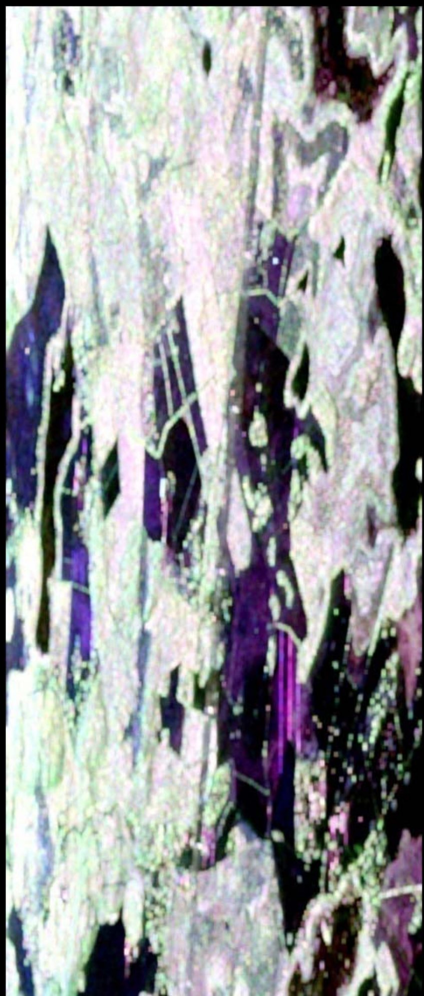

|HH+VV| |HV| |HH-VV|

$-2\ln\left(\Lambda^{\tau}_{RVoG}\right)$

RVoG hypoth.

No RVoG hypoth.

Data provided by ESA

L-band

|HH+VV| |HV| |HH-VV|

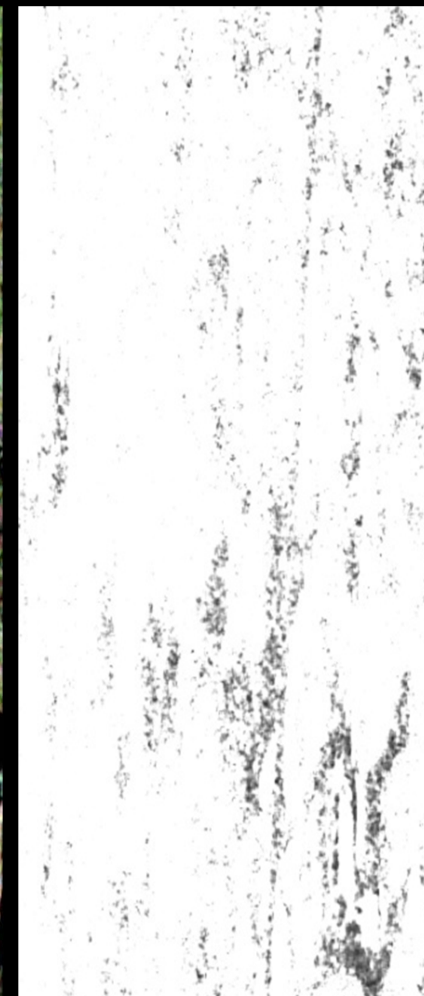

$-2\ln\left(\Lambda^{\tau}_{RVoG}\right)$

Results: Real PolInSAR Data

PolInSAR data: E-SAR BioSAR-1 Campaign Boreal Forest

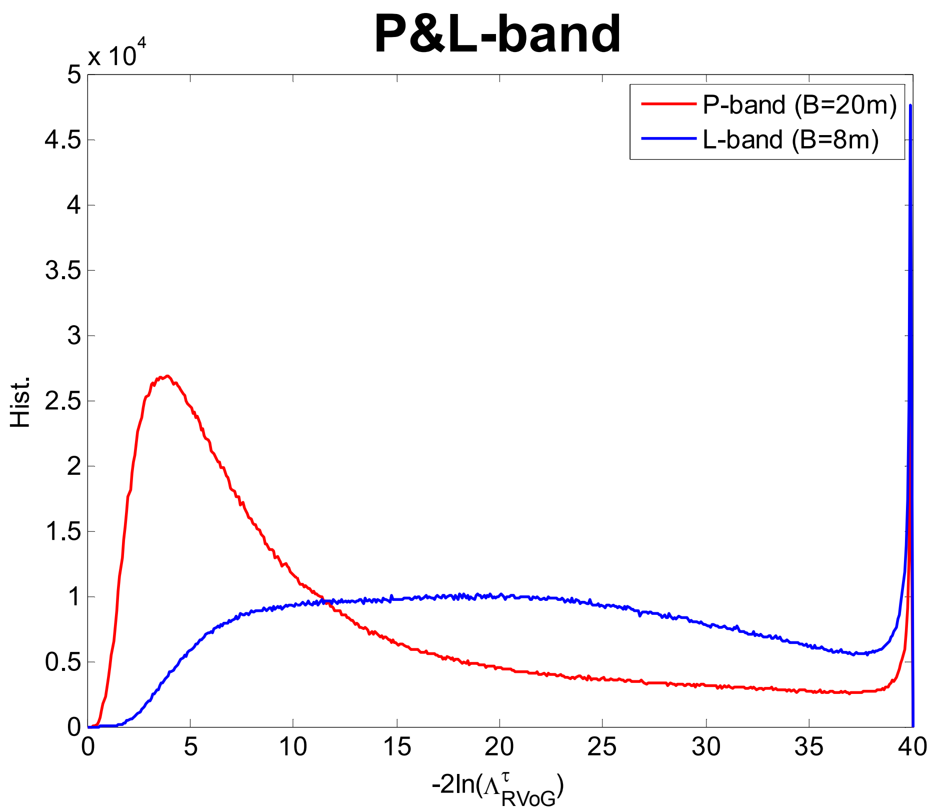

- The validity of the RVoG model hypothesis depends on the spatial baseline

Results: Real PolInSAR Data

PolInSAR data: Tropical vs. Boreal Forest

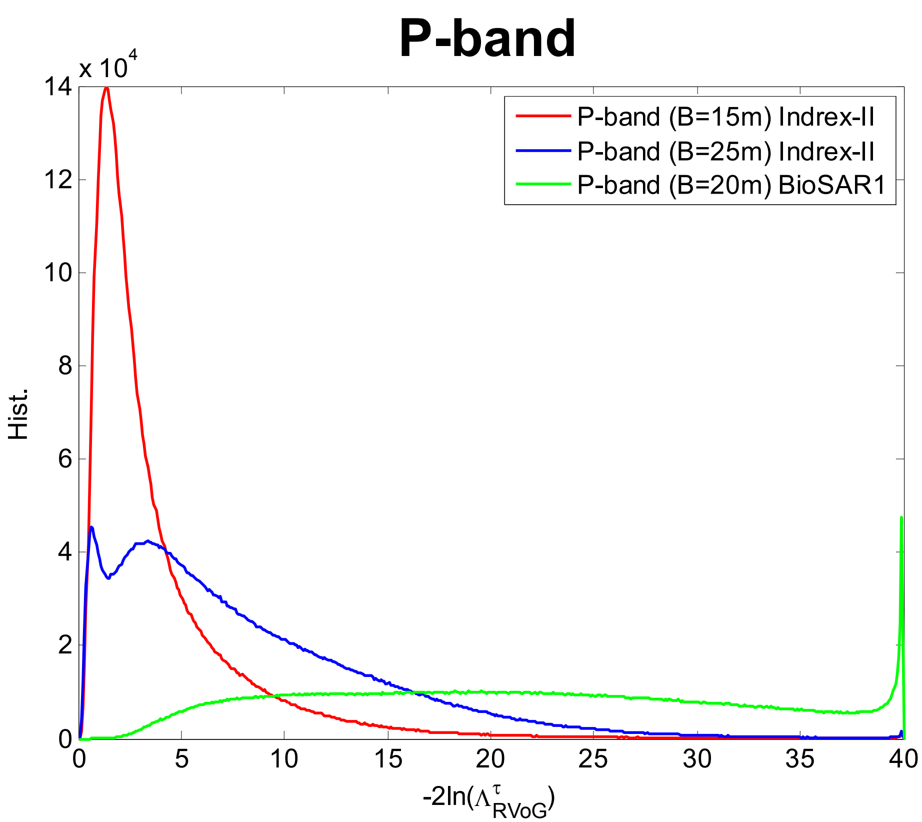

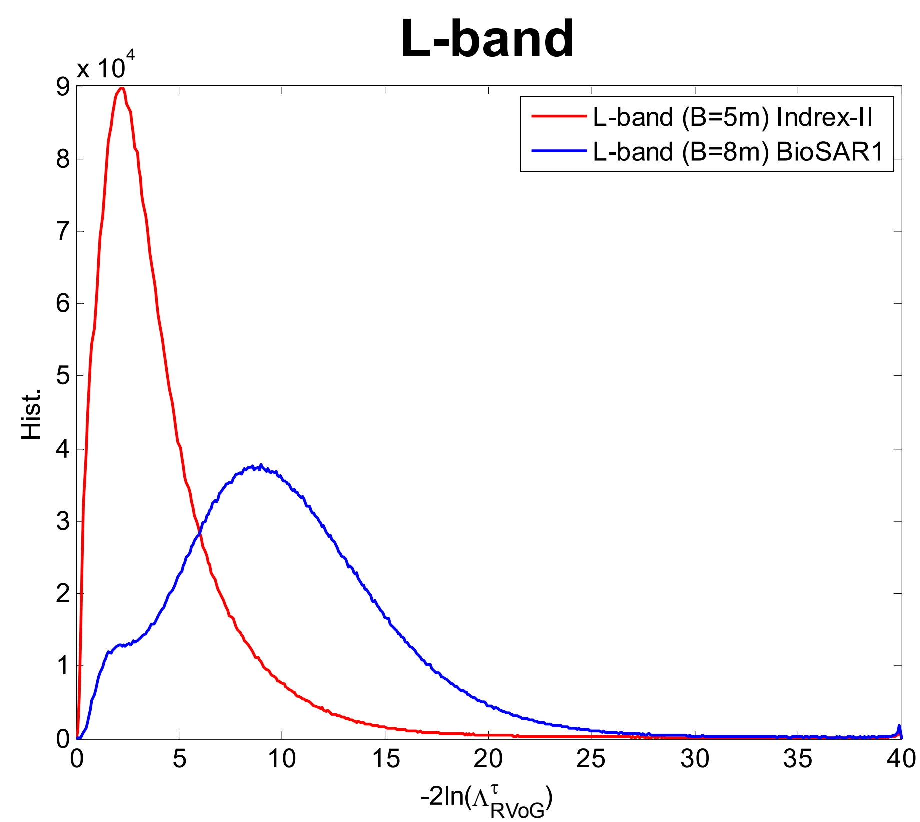

Conclusions

- Analysis of the RVoG model in PolInSAR data for the validation and estimation of the model
  - MLR provides a metric to compare the effect of any parameter on the validity of the RVoG model hypothesis
- Validation
  - The RVoG hypothesis is true if the normalized PolInSAR matrix $\tilde{\mathbf{\Omega}}_{12}$ is affine equivalent to an Hermitian matrix
    - Translations and rotations are insufficient in presence of speckle
  - Use of a ML approach to derive the GLRT for the RVoG hypothesis model analysis
- Estimation is SB-PolInSAR & MB-PolInSAR
  - Calculation of the ML estimator of the coherency matrix that makes data to fulfill the RVoG model
  - Estimation of the line segment of the RVoG and not only the line
- Results
  - RVoG validity depends on frequency and baseline
  - RVoG validity depends on incidence angle (ground-to-volume ratio?)
  - RVoG validity seems to be higher in Tropical than in Boreal forests

The Trace Matrix

The solution of the previous equations systems may be expressed in a matrix form

$$\underbrace{\begin{bmatrix} \mathrm{tr}(\mathbf{H}_1) & \mathrm{tr}(\mathbf{H}_2) & 3 \\ \mathrm{tr}(\mathbf{H}_1\mathbf{H}_2) & \mathrm{tr}(\mathbf{H}_2\mathbf{H}_2) & \mathrm{tr}(\mathbf{H}_2) \\ \mathrm{tr}(\mathbf{H}_1\mathbf{H}_1) & \mathrm{tr}(\mathbf{H}_2\mathbf{H}_1) & \mathrm{tr}(\mathbf{H}_1) \end{bmatrix}}_{\text{Trace matrix}} \begin{bmatrix} \Im\{a\} \\ \Re\{b\} \\ \Im\{c\} \end{bmatrix} = \begin{bmatrix} 0 \\ 0 \\ 0 \end{bmatrix} \Rightarrow \boxed{\Upsilon\mathbf{t} = \mathbf{0}}$$

- If CL applies, rank{Υ}=2, i.e., det{Υ}=0
  - Line parameters derived in

    L. Ferro-Famil, Y. Huang, M. Neumann, "Robust estimation of Multi-Baseline POL-inSAR parameters for the analysis of natural environments" EUSAR 2010
- If CL does not apply, rank{Υ}=3, i.e., det{Υ}$\neq$0

The rank of the Trace matrix indicates the validity of the CL hypothesis, i.e., the validity of the RVoG model

Continuous validity of the CL/RVoG model hypothesis based on the SVD decomposition of the trance matrix, based on the idea of the polarimetric Anisotropy

$$\sigma_1 \geq \sigma_2 \geq \sigma_3 \geq 0$$

Singular values of the Trace matrix

$$\Rightarrow \boxed{\Lambda^A_{RVoG} = \frac{\sigma_2 - \sigma_3}{\sigma_2 + \sigma_3}}$$

$$0 \leq \Lambda^A_{RVoG} \leq 1$$

RVoG hypothesis is not valid	RVoG hypothesis is valid

Results: Real PolInSAR Data

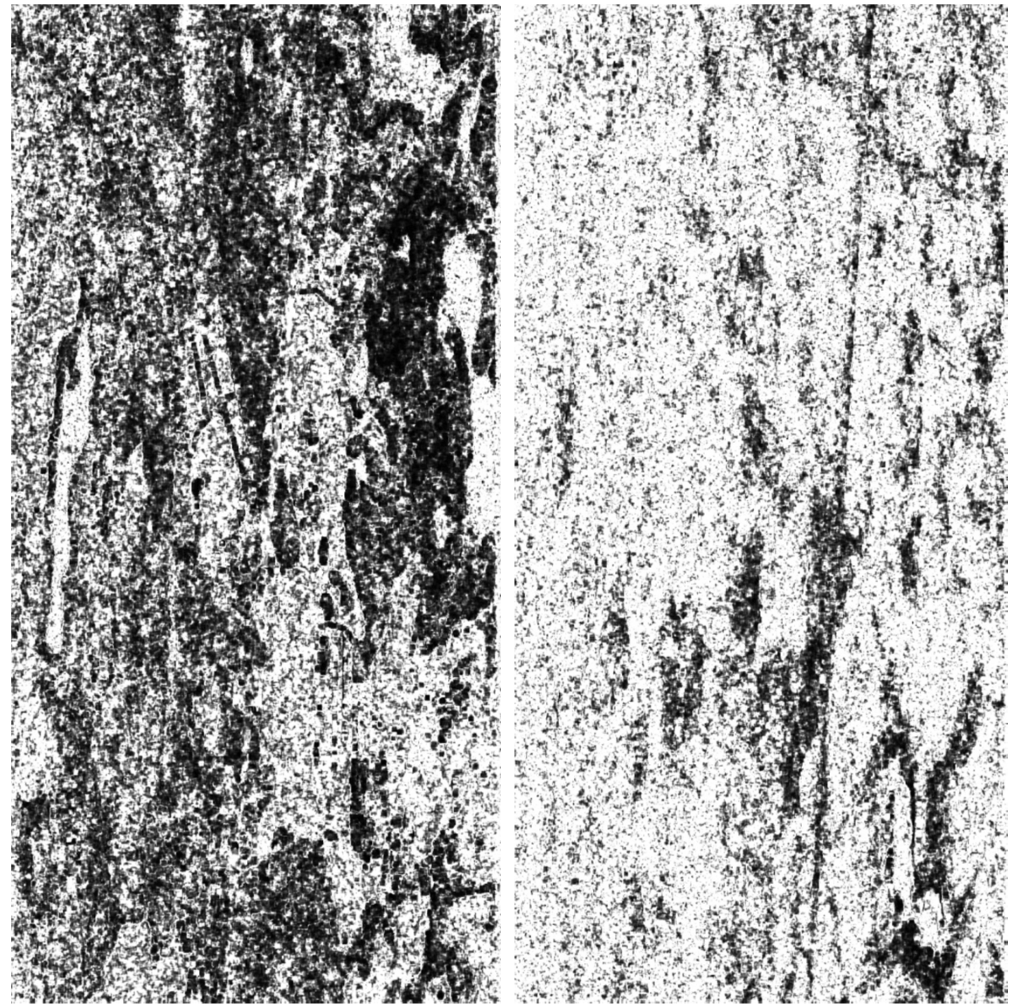

Simulated PolInSAR data

- Imaging systems: DLR's E-SAR
  - Range spatial resolution 1.5 m
  - Azimuth spatial resolution 1.5 m
  - Wavelength λ=0.23 m (L-band)
  - Flight height H=3000 m
  - Mean incidence angle θ=45 deg
- Simulated scenarios: Four different scenarios based on the RVoG model hypothesis

Scenario	Baseline [m]	h_v [m]	ϕ_1 [rad]	PS	CL
1	10	20	0	Yes	Yes
2	8	30	$\pi/2$	Yes	Yes
3	10	20	0	Yes	No
4	10	20	0	No	No

- Statistical distribution: Wishart pdf

Results: Simulated PolInSAR Data

Ratio's values

Scenario 1: PS & CL

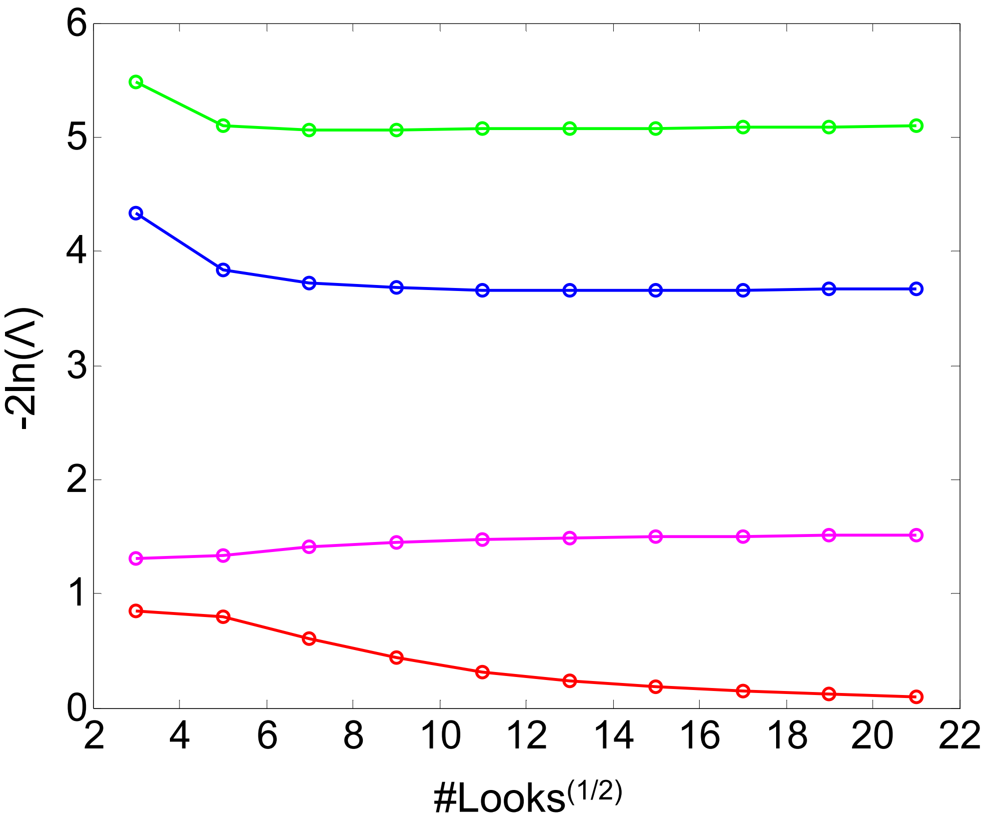

Scenario 2: PS & CL

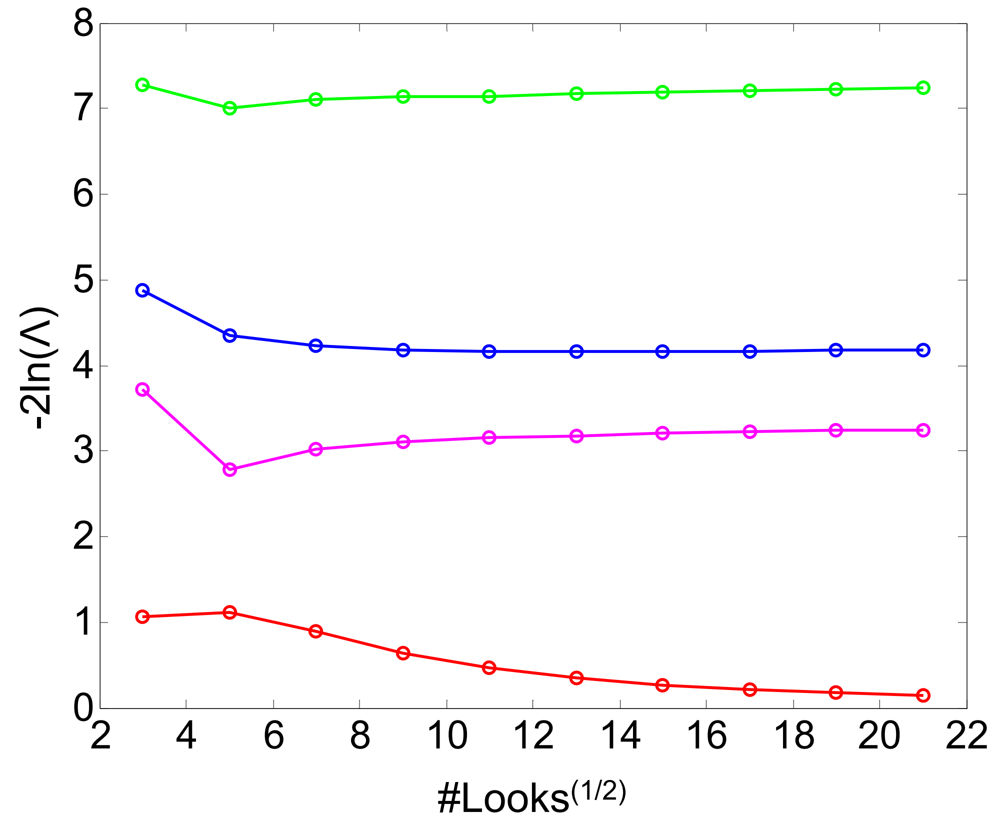

Λ^{τ}_{PS} **PS hypothesis**

Λ^{A}_{RVoG}

Λ^{τ}_{RVoG}

Λ^{τ}_{CL} **CL hypothesis**

Ratio's values

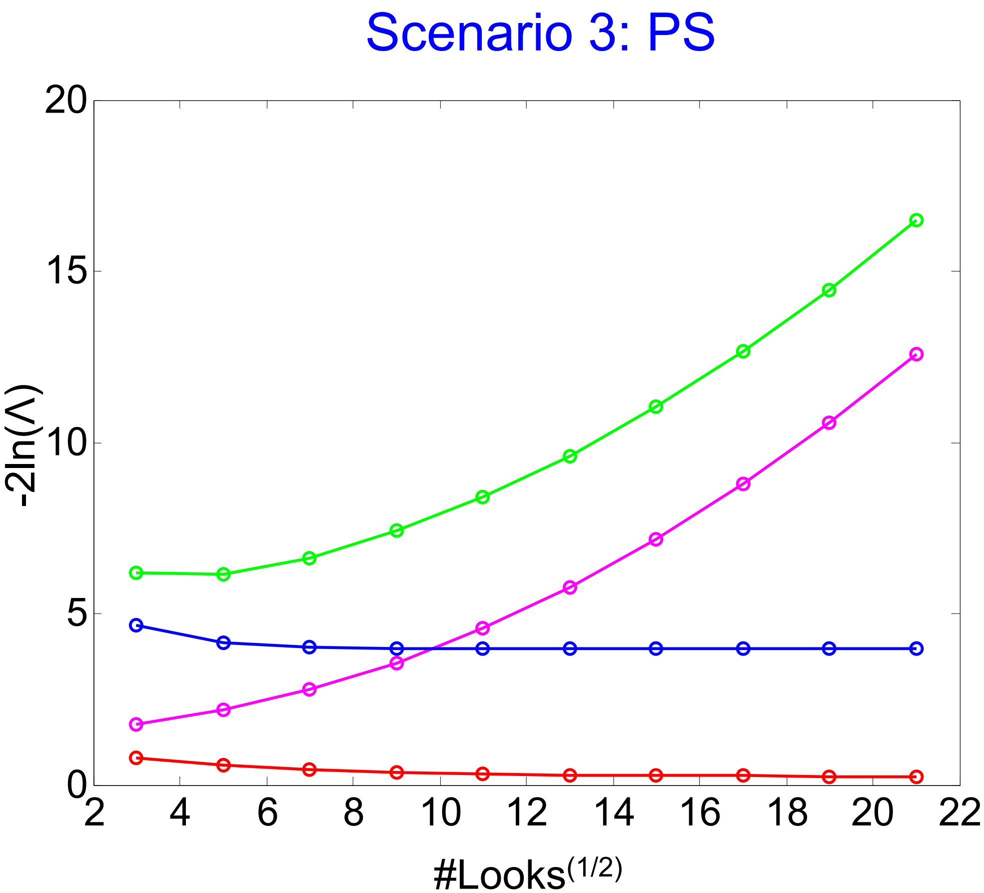

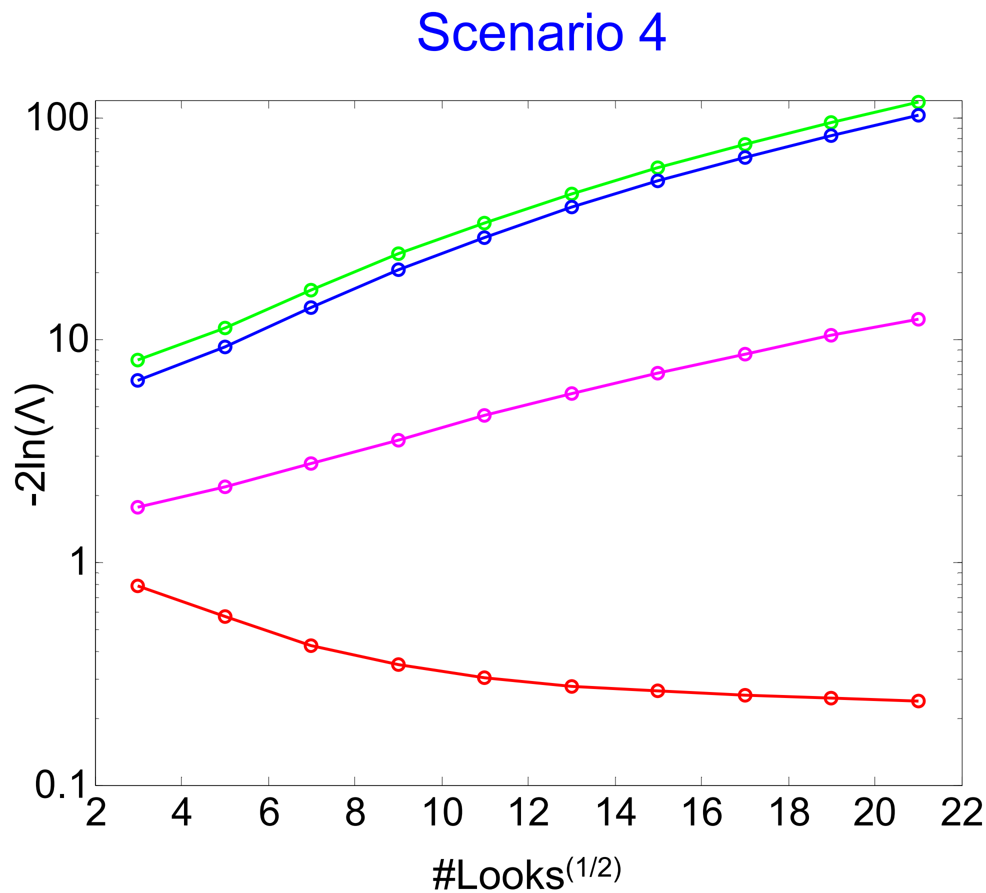

Λ^{A}_{RVoG} (red) Λ^{τ}_{RVoG} (green)

Λ^{τ}_{PS} (blue) **PS hypothesis**

Λ^{τ}_{CL} (magenta) **CL hypothesis**

Results: Simulated PolInSAR Data

Coherence regions from individual pixels

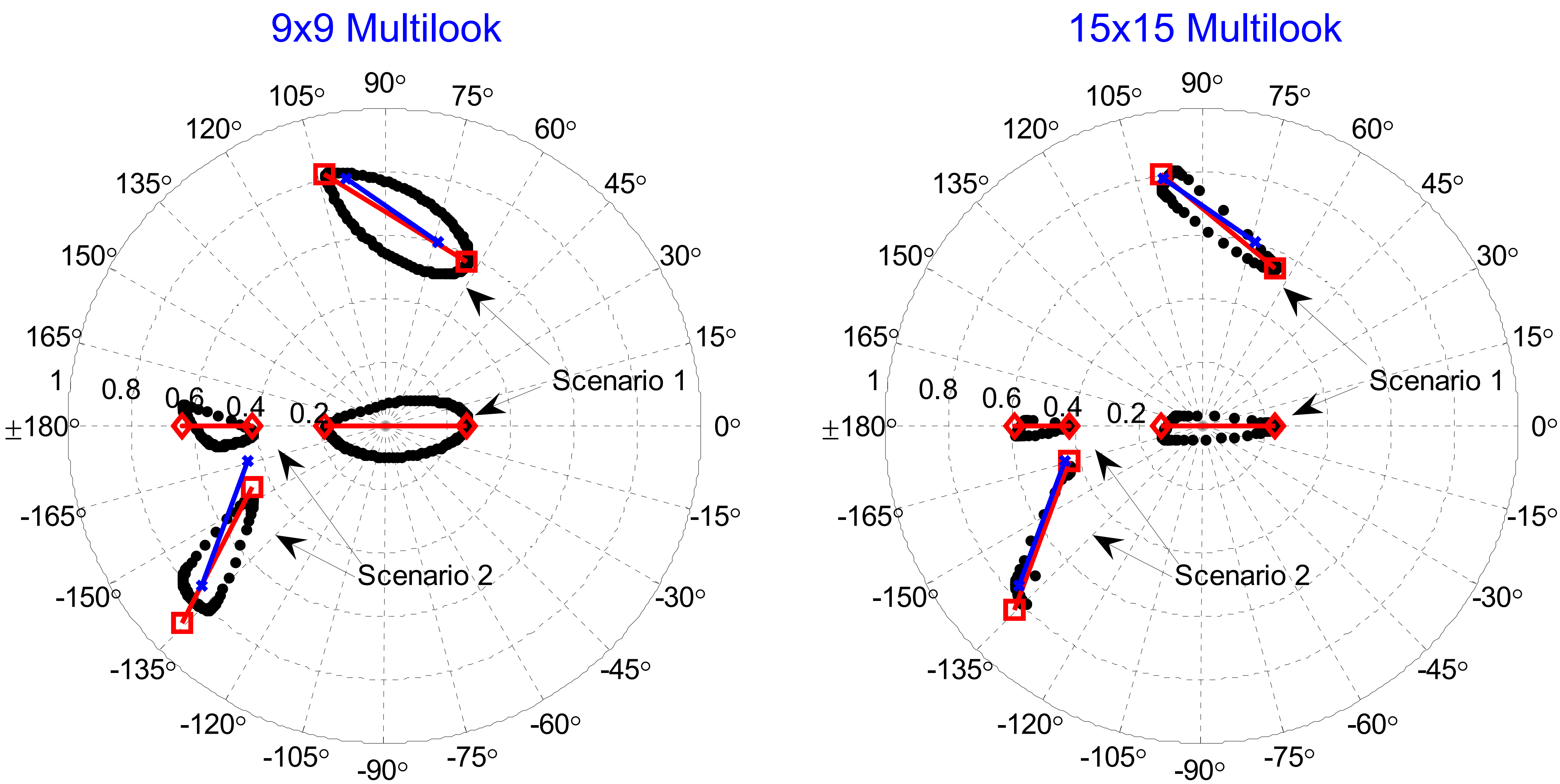

Theoretical CR

Estimated CR from multilook

Estimated CR from ML

Results: Real PolInSAR Data

Coherence regions from individual pixels